

Unified interpretation for second-order subwavelength interference based on Feynman's path-integral theory

Jianbin Liu* and Guoquan Zhang

The MOE Key Laboratory of Weak Light Nonlinear Photonics, Nankai University, Tianjin 300457, China and Photonics Center, School of Physics, Nankai University, Tianjin 300071, China

(Received 28 March 2010; published 21 July 2010)

The second-order spatial subwavelength interference pattern is observed in a modified Michelson interferometer with single-mode continuous-wave laser beams. By analyzing our subwavelength interference experiment based on Feynman's path integral theory, a unified interpretation for all the second-order subwavelength interference is suggested.

DOI: [10.1103/PhysRevA.82.013822](https://doi.org/10.1103/PhysRevA.82.013822)

PACS number(s): 42.50.Ar, 42.50.St

I. INTRODUCTION

The de Broglie wavelength of a particle is defined as $\lambda_B = h/p$, where h is the Planck constant and p is the magnitude of the particle's momentum [1]. Based on the definition, the de Broglie wavelength of a particle will decrease as its magnitude of momentum increases. If, in certain specific conditions, N identical but independent particles can be treated as a whole, the de Broglie wavelength of this N -particle entity is $h/(Np)$, which is only one N th of the de Broglie wavelength of a single particle.

Interference is a conventional way to measure de Broglie wavelength, and subwavelength interference often indicates that the de Broglie wavelength of several particles as a whole is measured [2–5]. The second-order subwavelength interference of light or two-photon de Broglie wavelength was first observed by using entangled photon pairs generated by Spontaneous Parametric Down-Conversion (SPDC) from a nonlinear crystal [6–12]. It was thought that subwavelength interference could be realized with entangled photons only. However, subwavelength interference with pseudothermal light [13–15] and coherent light [16–18] were also reported later. Therefore, subwavelength interference of photons is not a property for certain specific light only, but a general property of photons which can be observed with appropriate detection schemes.

The Hanbury Brown–Twiss (HBT) interferometer is usually employed to measure the second-order interference pattern, in which there are two detectors to measure the coincidence counts or correlations [19]. It is interesting to notice that the second-order spatial subwavelength interference can be observed when the two detectors are scanned either in the same direction [8–11,17,18] or in opposite directions [9,13–15].

From a mathematical point of view, the condition to observe the second-order subwavelength interference is to find a way to eliminate the first-order interference [3,20]. From a physical point of view, there are many different ways to meet this condition. Let us take Young's double-slit interferometer as an example, which is also employed in most of the reported second-order subwavelength interference experiments. One way to eliminate the first-order interference is to employ

entangled photons to ensure that the measured two photons go through the same slit to trigger the joint detection event [7–10], or one can achieve the same condition by using a special two-photon detector [21]. Another way is to use thermal or pseudothermal light, in which the first-order interference of light from different slits will disappear for a long time average when these two slits are in different coherence areas [13–15,22]. Laser light can also be employed by artificially changing the relative phase of the fields at these two slits to eliminate the first-order interference [17,23], which is also the condition we used to observe the second-order subwavelength interference pattern in our experiments.

The subwavelength interference experiments are explained by different interpretations, which can be divided into two categories: one is the multiphoton interference theory based on Glauber's quantum optical coherence theory [7,9,10,13,15,24], the other one is the intensity fluctuation correlation theory [14,17,18,25]. There is a hot debate about the physics behind the second- and high-order interference between these two different interpretations. For details about the debate, please refer to Refs. [26–28] and references therein. However, it is not the intention of this paper to enter this debate. In this paper, by analyzing the observed second-order spatial subwavelength interference of single-mode continuous-wave (cw) laser beams in a modified Michelson interferometer, we suggest a unified interpretation for all the second-order subwavelength interference experiments based on Feynman's path integral theory.

This paper is organized as follows. We will first introduce our subwavelength interference experiment in Sec. II, and then interpret the experimental results based on Feynman's path integral theory in Sec. III. Applying our interpretation to explain other second-order subwavelength interference experiments can be found in Sec. IV. Our conclusions are in Sec. V.

II. SUBWAVELENGTH INTERFERENCE WITH SINGLE-MODE CW LASER BEAMS

The experimental setup is shown in Fig. 1; it is a modified Michelson interferometer similar to the one used in our previous experiments [29]. A 780-nm single-mode cw laser with a 200-kHz frequency bandwidth is employed. A convex lens F with a focal length $f = 3.8$ mm is employed to focus the laser beam to simulate a point source S . A piezoelectric mirror (PM)

*ljb@mail.nankai.edu.cn

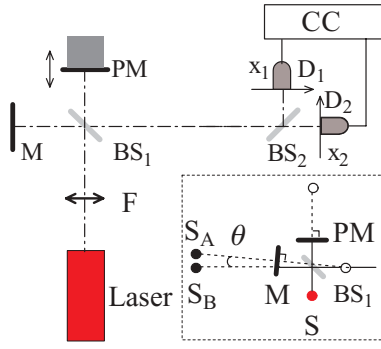


FIG. 1. (Color online) Modified Michelson interferometer. F : lens. M : mirror. PM : piezoelectric mirror. BS_j : nonpolarized 1:1 beam splitter ($j = 1$, and 2). D_j : single-photon detector ($j = 1$ and 2). CC : two-photon coincidence counting system. The inset shows the equivalent Young's double-point-source interferometer, where S_A and S_B are the image sources of the point source S . The angle θ has been enlarged to show the scheme clearly.

and a reflection mirror M are placed at the end of two arms of the interferometer, respectively. The PM is perpendicular to the light propagation direction. A 90-V, 100-Hz sinusoidal voltage signal is applied on the PM to make it shift repeatedly along the direction of light so that the phase shift between photons in these two arms changes continuously between $-\pi$ and π . BS_j and D_j ($j = 1$, and 2) are 1:1 nonpolarized beam splitter and single-photon detector, respectively. CC is a two-photon coincidence counting system which can record the single-photon counting rates and the coincidence counting rate of D_1 and D_2 simultaneously. Note that the angle between M and PM is $\pi/2 + \theta$ with $\theta = 4.3$ mrad, therefore, the whole setup works as a Young's double-point-source interferometer shown in the inset of Fig. 1. The distance d between these two virtual point sources S_A and S_B is 1.815 mm and the distance L between the source and the detection planes is 1862 mm.

The experimental results are shown in Figs. 2–4. The single-photon counting rates of D_1 and D_2 in Figs. 2(a), 3(a), and 4(a) show that the first-order interference patterns are not observable, which has been confirmed by the measurement of a CCD in our previous experiments [29]. The normalized second-order coherence functions $g^{(2)}$ at various experimental conditions are shown in Figs. 2(b), 3(b), and 4(b), where the diamond dots are the measured results and the solid curves are the theoretical simulations by employing the equations below. The second-order interference pattern in Fig. 2(b) is acquired by fixing D_2 and scanning D_1 along x_1 direction in the detection plane. The periodicity and visibility are $800 \mu\text{m}$ and $(46 \pm 2)\%$, respectively. The second-order interference pattern in Fig. 3(b) is acquired by scanning D_1 and D_2 in opposite directions. The periodicity and visibility are $400 \mu\text{m}$ and $(48 \pm 4)\%$, respectively. Note that the periodicity Λ of the interference pattern, and the inferred wavelength λ_B , are connected by $\lambda_B = (d/L) \cdot \Lambda$ (see below). The measured two-photon wavelength λ_B in Fig. 3(b) is 390 nm, which is exactly half of the wavelength of the employed laser. Hence the results of Fig. 3(b) indicate the appearance of second-order subwavelength interference. The

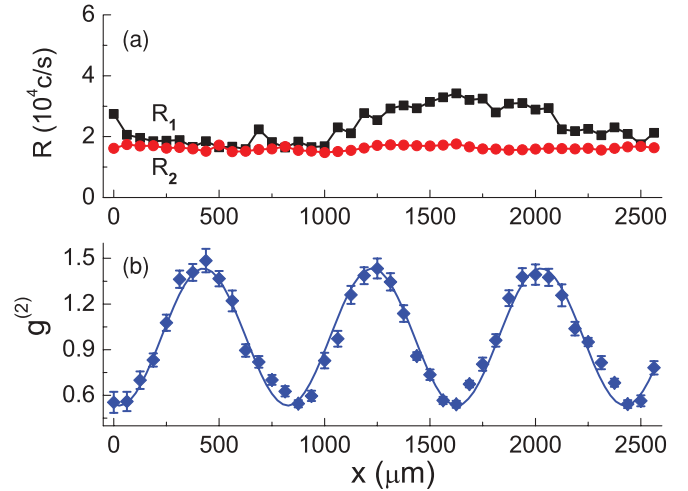


FIG. 2. (Color online) Normal second-order interference pattern when D_1 is scanned along x_1 direction and D_2 is fixed. (a) The black square and red circle dots are single-photon counting rates of D_1 and D_2 , respectively. (b) The blue diamond dots are experimental results of the measured normalized second-order coherence function and the blue solid curve is a theoretical fit by using Eq. (9) with a periodicity of $800 \mu\text{m}$.

normalized second-order coherence function in Fig. 4(b) is a constant, 0.55 ± 0.04 , when these two detectors D_1 and D_2 are scanned in the same direction. The measurements show that the value of the normalized second-order coherence function in this case is dependent only on the initial relative positions of these two detectors, within a range approximately from 0.5 to 1.5.

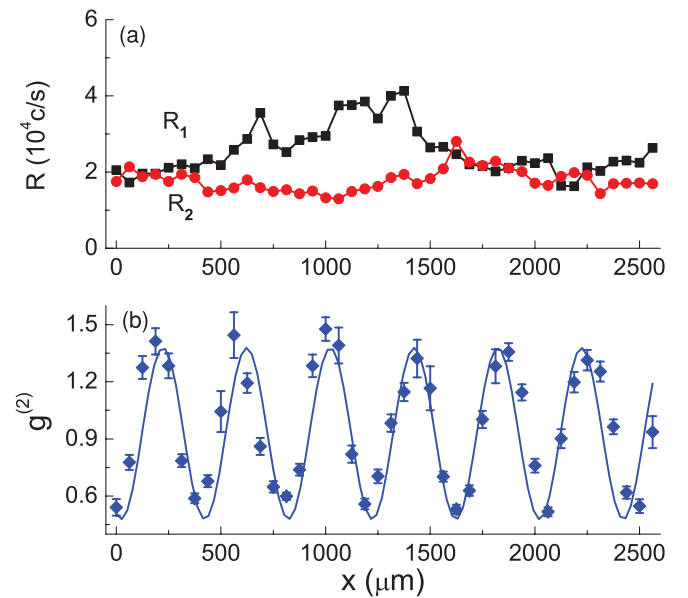


FIG. 3. (Color online) Second-order subwavelength interference pattern when D_1 and D_2 are scanned in opposite directions. (a) The black square and red circle dots are single-photon counting rates of D_1 and D_2 , respectively. (b) The blue diamond dots are experimental results of the measured normalized second-order coherence function and the blue solid curve is a theoretical fit by using Eq. (10) with a periodicity of $400 \mu\text{m}$.

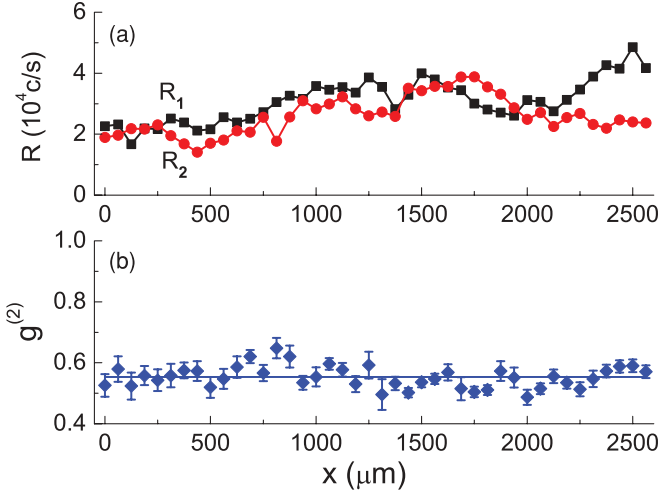


FIG. 4. (Color online) Constant second-order interference pattern when D_1 and D_2 are scanned in the same direction. (a) The black square and red circle dots are single-photon counting rates of D_1 and D_2 , respectively. (b) The blue diamond dots are experimental results of the measured normalized second-order coherence function and the blue solid line is a theoretical fit by using Eq. (11).

III. TWO-PHOTON INTERFERENCE BASED ON FEYNMAN'S PATH INTEGRAL THEORY

In this section, we will calculate the two-photon probability distribution based on Feynman's path integral theory. However, before the formal calculation for our experiments, it is important to point out the difference between the multiphoton interference theory based on Glauber's optical coherence theory and that based on Feynman's path integral theory.

The starting point of Glauber's optical coherence theory to solve a problem is the famous definition of optical coherence function based on the photon detection model [24]. With further mathematical calculation by considering the field operators and the wave function of the system, one may conclude that the N th-order ($N \geq 1$) interference of light is a result of N -photon interference. For instance, we have done this job for thermal light [30]. This process may become cumbersome when the wave function of the system is complicated. However, based on Feynman's path integral theory, we can directly write out all possible ways to trigger photon detection events and calculate the corresponding probability distributions. The wave function of the system is not necessary if the phase and number distributions of photons are known, which may simplify some problems significantly. Of course, both Glauber's optical coherence theory and Feynman's path integral theory belong to quantum electrodynamics. There should be no difference in principle between these two interpretations. They are two different ways to reach the same destination.

In the following, we will interpret the observed second-order interference phenomena in Sec. II based on Feynman's path integral theory. In order to follow the tradition, we will use the symbols defined by Glauber [24]. For simplicity, we suppose that the two point sources, S_A and S_B , have equal probability to emit photons. The emitted photons may be correlated or independent, depending on what kind of light

is employed. Based on Feynman's path integral theory, the second-order coherence function can be expressed as [31]

$$G^{(2)}(\mathbf{r}_1, t_1; \mathbf{r}_2, t_2) = \langle |e^{i\varphi_A} e^{i\varphi_B} g_{A1} g_{B2} + e^{i\varphi_A} e^{i\varphi_B} g_{A2} g_{B1} + e^{i\varphi'_A} e^{i\varphi'_A} g_{A1} g_{A2} + e^{i\varphi'_B} e^{i\varphi'_B} g_{B1} g_{B2}|^2 \rangle, \quad (1)$$

where $\langle \dots \rangle$ means ensemble average, i.e., taking all possible realizations of these different paths into account. For a stationary and ergodic process, the ensemble average is equivalent to a time average over a long period [32]. (\mathbf{r}_1, t_1) and (\mathbf{r}_2, t_2) are the space-time coordinates for the photon detection events at D_1 and D_2 , respectively. φ_α , φ'_α , and φ''_α are initial phases of different photons emitted by S_α ($\alpha = A$ and B). $g_{\alpha\beta}$ is Feynman's photon propagator that describes a photon emitted by S_α and detected at D_β ($\alpha = A$ and B , $\beta = 1$ and 2).

For the point source in our experiments, Feynman's photon propagator can be expressed as [33]

$$g_{\alpha\beta} = \frac{\exp[-i(\mathbf{k}_{\alpha\beta} \cdot \mathbf{r}_{\alpha\beta} - \omega_{\alpha\beta} t_{\alpha\beta})]}{r_{\alpha\beta}}, \quad (2)$$

which is the same as the Green function for a point source in classical optics [34]. $\mathbf{k}_{\alpha\beta}$ and $\mathbf{r}_{\alpha\beta}$ are the wave and position vectors of the photon emitted by S_α and detected at D_β , respectively. $r_{\alpha\beta} = |\mathbf{r}_{\alpha\beta}|$ is the distance between S_α and D_β . $\omega_{\alpha\beta}$ and $t_{\alpha\beta}$ are the frequency and time for the photon that is emitted by S_α and detected at D_β , respectively. There are four different yet indistinguishable ways for a measured photon pair to trigger a two-photon joint detection event in Eq. (1). For example, the first term on the right-hand side of Eq. (1) represents the probability amplitude for a photon pair to trigger a coincidence count when one of the photons has traveled from S_A to D_1 while the other has traveled from S_B to D_2 . The other three terms in Eq. (1) are defined similarly.

In our experiments, within the coincidence time window (4.88 ns), the phase relation can be approximated as [29]

$$\begin{aligned} \varphi_A &= \varphi'_A = \varphi''_A = 0, \\ \varphi_B &= \varphi'_B = \varphi''_B = \varphi, \end{aligned} \quad (3)$$

where φ is the phase shift between the photons emitted by S_A and S_B . For a long time interval, it satisfies the condition [29]

$$\langle e^{i\varphi} \rangle = 0. \quad (4)$$

The frequency bandwidth of the single-mode cw laser is 200 kHz, thus it is proper to treat it as single frequency light. Therefore we will drop the temporal parts of light related with the term ωt in the following discussions.

Substituting Eqs. (2)–(4) into Eq. (1), it is easy to get

$$G^{(2)}(\mathbf{r}_1, \mathbf{r}_2) = \frac{4}{r^4} \left\{ 1 + \frac{1}{2} \cos[(\mathbf{k}_{A1} \cdot \mathbf{r}_{A1} - \mathbf{k}_{B1} \cdot \mathbf{r}_{B1}) - (\mathbf{k}_{A2} \cdot \mathbf{r}_{A2} - \mathbf{k}_{B2} \cdot \mathbf{r}_{B2})] \right\}, \quad (5)$$

where the approximation $r_{\alpha\beta} \approx r_\beta \sim r$ ($\alpha = A$ and B , $\beta = 1$ and 2) has been employed to simplify Eq. (5), in which r_β is the distance between the center of the two point sources and D_β . This approximation is valid when the distance d between the two point sources is much smaller than the distance L between the source and the detection planes [34].

The normalized second-order coherence function, $g^{(2)}(x_1, x_2)$, is related with the second-order coherence function, $G^{(2)}(x_1, x_2)$, by [24]

$$g^{(2)}(x_1, x_2) = \frac{G^{(2)}(x_1, x_2)}{G^{(1)}(x_1)G^{(1)}(x_2)}, \quad (6)$$

where $G^{(1)}(x_i)$ ($i = 1$ and 2) is the first-order coherence function and can also be calculated based on Feynman's path integral theory [31]

$$G^{(1)}(x_i) = \langle |e^{i\varphi_A} g_{Ai} + e^{i\varphi_B} g_{Bi}|^2 \rangle. \quad (7)$$

Substituting Eqs. (1)–(4) and (7) into (6) and with the paraxial approximations $d \ll L$ and $x_{max} \ll L$ (x_{max} is the maximum transverse position of the detector in the detection plane), the normalized second-order coherence function in the one-dimensional case can be simplified as [29,34]

$$g^{(2)}(x_1, x_2) = 1 + \frac{1}{2} \cos \frac{kd}{L}(x_1 - x_2), \quad (8)$$

where $k = |\mathbf{k}_{\alpha\beta}|$ is the magnitude of the wave vector and is independent of the subscripts α and β . This is because both of the two virtual point sources S_A and S_B originate from the same point source S and therefore the photons are of the same wavelength. x_1 and x_2 are the transverse coordinates of D_1 and D_2 in the detection planes, respectively.

If we scan D_1 along x_1 and fix D_2 , i.e., $x_1 = a + x$ and $x_2 = b$, where a and b are the initial positions of D_1 and D_2 , respectively, Eq. (8) can be expressed as

$$g^{(2)}(x) = 1 + \frac{1}{2} \cos \frac{kd}{L}(x + a - b). \quad (9)$$

The theoretical period of the interference pattern is $800 \mu\text{m}$ by taking the experimental parameters into account. The maximal theoretical visibility is 50%, which is consistent with the observed interference pattern in Fig. 2(b).

If we scan the two detectors in opposite directions as $x_1 = a + x$ and $x_2 = b - x$, Eq. (8) can be simplified as

$$g^{(2)}(x) = 1 + \frac{1}{2} \cos \frac{kd}{L}(2x + a - b). \quad (10)$$

The theoretical period of Eq. (10) is $400 \mu\text{m}$, which is half of the one in Eq. (9) and therefore indicates the appearance of subwavelength interference. The maximum visibility of the interference pattern is again 50%. Once again, the theoretical simulation is in good agreement with the experimental results in Fig. 3(b).

When the two detectors are scanned in the same direction as $x_1 = a + x$ and $x_2 = b + x$, the normalized second-order coherence function becomes

$$g^{(2)}(x) = 1 + \frac{1}{2} \cos \frac{kd}{L}(a - b) \sim \text{const.} \quad (11)$$

The value of $g^{(2)}(x)$ is dependent only on the initial position difference of the two detectors, as confirmed by the experimental observations shown in Fig. 4(b).

IV. DISCUSSIONS

To take a deep insight about the second-order subwavelength interference, one has to consider the general case of second-order coherence, in which all 16 terms in Eq. (1) remain

after ensemble average. This can be achieved, for example, when the phase relation satisfies

$$\varphi_A = \varphi'_A = \varphi''_A = \varphi_B = \varphi'_B = \varphi''_B, \quad (12)$$

which can be realized experimentally, for instance, when the two point sources are originated from the same single-mode cw laser without introducing any phase shift between them. In the following, we will show that, in all the reported second-order subwavelength interference experiments (including ours), one keeps only part of these 16 terms by satisfying some special conditions, such as using entangled photon pairs [6–12], employing pseudothermal light sources in different coherence areas [13–15], or introducing phase changes between two point sources in lasers [17,18].

Substituting Eqs. (2) and (12) into Eq. (1), we find (only considering the spatial part)

$$\begin{aligned} G^{(2)}(\mathbf{r}_1, \mathbf{r}_2) \propto & 4 + 4 \cos(\mathbf{k}_{A1} \cdot \mathbf{r}_{A1} - \mathbf{k}_{B1} \cdot \mathbf{r}_{B1}) \\ & + 4 \cos(\mathbf{k}_{A2} \cdot \mathbf{r}_{A2} - \mathbf{k}_{B2} \cdot \mathbf{r}_{B2}) \\ & + 2 \cos[(\mathbf{k}_{A1} \cdot \mathbf{r}_{A1} - \mathbf{k}_{B1} \cdot \mathbf{r}_{B1}) \\ & - (\mathbf{k}_{A2} \cdot \mathbf{r}_{A2} - \mathbf{k}_{B2} \cdot \mathbf{r}_{B2})] \\ & + 2 \cos[(\mathbf{k}_{A1} \cdot \mathbf{r}_{A1} - \mathbf{k}_{B1} \cdot \mathbf{r}_{B1}) \\ & + (\mathbf{k}_{A2} \cdot \mathbf{r}_{A2} - \mathbf{k}_{B2} \cdot \mathbf{r}_{B2})]. \end{aligned} \quad (13)$$

The first term of the right-hand side of Eq. (13) is a constant that gives the accidental two-photon coincidence counts. The second and third terms are due to the first-order interference, and the last two terms are the pure second-order interference which can be used to realize the second-order subwavelength interference. A more detailed analysis reveals that the fourth term originates from the interference between $g_{A1}g_{B2}$ and $g_{A2}g_{B1}$, while the fifth term is caused by the interference between $g_{A1}g_{A2}$ and $g_{B1}g_{B2}$. There is no difference in principle between the fourth and fifth terms on the right-hand side of Eq. (13), for both of them are the superposition of two-photon probability amplitudes corresponding to different yet indistinguishable ways for a measured photon pair to trigger a coincidence count event.

Within the same paraxial approximation as Eq. (8) and considering the one-dimensional case, Eq. (13) can be further simplified as

$$\begin{aligned} G^{(2)}(x_1, x_2) \propto & 4 + 4 \cos \frac{kd}{L}x_1 + 4 \cos \frac{kd}{L}x_2 \\ & + 2 \cos \frac{kd}{L}(x_1 - x_2) + 2 \cos \frac{kd}{L}(x_1 + x_2). \end{aligned} \quad (14)$$

It is evident that the fourth term on the right-hand side of Eq. (14) will give subwavelength interference when the two detectors are scanned in opposite directions, and the fifth term will give subwavelength interference when the two detectors are scanned in the same direction. The remaining problem to observe the second-order subwavelength interference is to keep one of these two terms by eliminating the other unwanted terms with proper arrangements.

Armed with Eq. (14) and the discussions above, we are ready to give a unified interpretation for the second-order spatial subwavelength interference based on Feynman's path integral theory. Taking the experiments in Ref. [9] as an

example, they observed subwavelength interference patterns with entangled photon pairs when the two detectors were scanned either in the same direction or in opposite directions by changing the profile of the pump beam for SPDC. As already pointed out by Fonseca *et al.* in Ref. [9], with a wire in the pump beam, it is possible to force an entangled photon pair to go through the same slit and to trigger a coincidence count event. Therefore, only the last two terms in Eq. (1), which result in the fifth term on the right-hand side of Eq. (14), contribute to the second-order interference. In this case, the two detectors must be scanned in the same direction to observe the subwavelength interference, which is consistent with the experimental results in Ref. [9]. Other experiments with entangled photon pairs in Refs. [7,10,11] also achieved the same condition with different methods.

When there is no wire in the pump beam, most of the measured photon pair will not go through the same slit, which means the fourth term on the right-hand side of Eq. (14) will dominate the second-order subwavelength interference. In this case, the subwavelength interference can be observed only when the two detectors are scanned in opposite directions, which is also consistent with the experimental results in Ref. [9]. All experiments with pseudothermal light [13–15] and our experiments with single-mode laser beams belong to this situation.

There is no such requirement for the two detectors to be scanned in opposite directions to observe the subwavelength interference for thermal or laser light. Similar to the case of entangled photon pairs, if there is a way to make the only possible ways to trigger a joint detection event be the last two terms in Eq. (1) or make the first two terms on the right-hand side of Eq. (1) have a π -phase difference, the subwavelength interference with thermal or laser light will also be observed when the two detectors are scanned in the same direction. For instance, the subwavelength interference patterns observed by Bentley *et al.* [17] and Pe'er *et al.* [18], respectively, are equivalent to scanning the two detectors in the same direction. The reason why we emphasize the case for the two detectors scanning in the same direction to get the subwavelength interference is that it can be used to increase the resolution of the lithography by using two-photon sensitive materials [3,10,17,18,21], while the case for the two detectors scanning in opposite directions cannot. However, there is no difference in principle between these two different situations as discussed above.

The second-order temporal subwavelength interference experiments can also be understood in the same way as the spatial ones. For instance, the second-order temporal subwavelength

interference in a Mach-Zehnder interferometer was observed only when the entangled photons were forced to follow the same path [6,7]. To the best of our knowledge, the second-order temporal subwavelength interference has been observed with entangled photon pairs only. By analogy to the second-order spatial subwavelength interference, it is reasonable to expect that the second-order temporal subwavelength interference can also be realized with thermal and laser light.

The discussions for the second-order subwavelength interference above can be easily generalized to the third- and higher-order subwavelength interference [17,35–38]. Furthermore, the multiphoton interference theory based on Feynman's path integral theory can also be used to discuss the interference of massive particles by using the proper Feynman's propagators [39–42].

V. CONCLUSION

In conclusion, we have reported a second-order spatial subwavelength interference experiment with single-mode cw laser beams in a modified Michelson interferometer. The measured two-photon de Broglie wavelength in our experiment is 390 nm, which is exactly half of the wavelength of the employed single-mode cw laser light. Two-photon interference theory based on Feynman's path integral theory has been employed to interpret the observed second-order subwavelength interference.

Furthermore, we have suggested that all the second-order subwavelength interference experiments, no matter what kind of light is employed, can be interpreted by the two-photon interference theory based on Feynman's path integral theory. Therefore the subwavelength interference of light is a general property of photons, and can be realized with proper arrangements. Both the spatial and temporal second-order subwavelength interferences can be realized with all kinds of light by employing appropriate arrangements. There is no difference in principle between the cases when the two detectors are scanned in the same direction and in opposite directions to observe the second-order subwavelength interference.

ACKNOWLEDGMENTS

The authors acknowledge the helpful discussions from Y. H. Shih. This project is supported by the MOE Cultivation Fund of the Key Scientific and Technical Innovation Project (708022), the NSFC (90922030, 10904077, 10804054), the 111 project (B07013), the 973 program (2007CB307002), the CNKBRSF (2006CB921703), and the RFDP (200800551034).

-
- [1] C. Cohen-Tannoudji, B. Diu, and F. Laloë, *Quantum Mechanics*, Vol. 1 (Wiley, New York, 1991).
 [2] J. Jacobson, G. Björk, I. Chuang, and Y. Yamamoto, *Phys. Rev. Lett.* **74**, 4835 (1995).
 [3] A. N. Boto, P. Kok, D. S. Abrams, S. L. Braunstein, C. P. Williams, and J. P. Dowling, *Phys. Rev. Lett.* **85**, 2733 (2000); D. V. Strekalov and J. P. Dowling, *J. Mod. Opt.* **49**, 519 (2002).

- [4] G. S. Agarwal, R. W. Boyd, E. M. Nagasako, and S. J. Bentley, *Phys. Rev. Lett.* **86**, 1389 (2001).
 [5] O. Steuernagel, *Phys. Rev. A* **65**, 033820 (2002).
 [6] J. G. Rarity, P. R. Tapster, E. Jakeman, T. Larchuk, R. A. Campos, M. C. Teich, and B. E. A. Saleh, *Phys. Rev. Lett.* **65**, 1348 (1990); T. S. Larchuk, R. A. Campos, J. G. Rarity, P. R. Tapster, E. Jakeman, B. E. A. Saleh, and M. C. Teich, *ibid.* **70**, 1603 (1993).

- [7] Y. H. Shih, A. V. Sergienko, M. H. Rubin, T. E. Kiess, and C. O. Alley, *Phys. Rev. A* **49**, 4243 (1994).
- [8] E. J. S. Fonseca, C. H. Monken, and S. Pádua, *Phys. Rev. Lett.* **82**, 2868 (1999).
- [9] E. J. S. Fonseca, Z. Paulini, P. Nussenzveig *et al.*, *Phys. Rev. A* **63**, 043819 (2001).
- [10] M. D'Angelo, M. V. Chekhova, and Y. H. Shih, *Phys. Rev. Lett.* **87**, 013602 (2001).
- [11] K. Edamatsu, R. Shimizu, and T. Itoh, *Phys. Rev. Lett.* **89**, 213601 (2002).
- [12] F. DeMartini, F. Sciarrino, C. Vitelli, R. G. Glasser, H. Cable, and J. P. Dowling, *Phys. Rev. A* **77**, 012324 (2008).
- [13] G. Scarcelli, A. Valencia, and Y. H. Shih, *Europhys. Lett.* **68**, 618 (2004).
- [14] K. G. Wang and D. Z. Cao, *Phys. Rev. A* **70**, 041801(R) (2004); J. Xiong, D. Z. Cao, F. Huang, H. G. Li, X. J. Sun, and K. Wang, *Phys. Rev. Lett.* **94**, 173601 (2005).
- [15] Y. H. Zhai, X. H. Chen, and L. A. Wu, *Phys. Rev. A* **74**, 053807 (2006).
- [16] D. V. Korobkin and E. Yablonovitch, *Opt. Eng.* **41**, 1729 (2002).
- [17] S. J. Bentley and R. W. Boyd, *Opt. Express* **12**, 5735 (2004).
- [18] A. Pe'er, B. Dayan, M. Vucelja *et al.*, *Opt. Express* **12**, 6600 (2004).
- [19] R. H. Brown and R. Q. Twiss, *Nature (London)* **177**, 27 (1956); **178**, 1046 (1956).
- [20] E. Yablonovitch and R. B. Vrijen, *Opt. Eng.* **38**, 334 (1999).
- [21] P. R. Hemmer, A. Muthukrishnan, M. O. Scully, and M. S. Zubairy, *Phys. Rev. Lett.* **96**, 163603 (2006).
- [22] W. Martienssen and E. Spiller, *Am. J. Phys.* **32**, 919 (1964).
- [23] I. N. Agafonov, M. V. Chekhova, T. Sh. Iskhakov, and A. N. Penin, *Phys. Rev. A* **77**, 053801 (2008).
- [24] R. J. Glauber, *Phys. Rev.* **130**, 2529 (1963); **131**, 2766 (1963).
- [25] A. Gatti, E. Brambilla, M. Bache, and L. A. Lugiato, *Phys. Rev. A* **70**, 013802 (2004); *Phys. Rev. Lett.* **93**, 093602 (2004).
- [26] A. Gatti, M. Bache, D. Magatti, E. Brambilla *et al.*, *J. Mod. Opt.* **53**, 739 (2006).
- [27] B. I. Erkmen and J. H. Shapiro, *Phys. Rev. A* **77**, 043809 (2008).
- [28] Y. H. Shih, e-print [arXiv:0805.1166v5](https://arxiv.org/abs/0805.1166v5).
- [29] J. B. Liu and G. Q. Zhang (submitted for publication).
- [30] J. B. Liu and Y. H. Shih, *Phys. Rev. A* **79**, 023819 (2009).
- [31] R. P. Feynman and A. R. Hibbs, *Quantum Mechanics and Path Integral* (McGraw-Hill, Inc., New York, 1965).
- [32] L. Mandel and E. Wolf, *Optical Coherence and Quantum Optics* (Cambridge University Press, New York, 1995).
- [33] M. E. Peskin and D. V. Schroeder, *An Introduction to Quantum Field Theory* (Westview Press, Colorado, 1995).
- [34] M. Born and E. Wolf, *Principles of Optics*, 7th ed. (Cambridge University Press, Cambridge, 1999).
- [35] M. W. Mitchell, J. S. Lundeen, and A. M. Steinberg, *Nature (London)* **429**, 161 (2004).
- [36] P. Walther, J. W. Pan, M. Aspelmeyer *et al.*, *Nature (London)* **429**, 158 (2004).
- [37] Z. Zhao, Y. A. Chen, A. N. Zhang *et al.*, *Nature (London)* **430**, 54 (2004).
- [38] C. Thiel, T. Bastin, J. Martin, E. Solano, J. von Zanthier, and G. S. Agarwal, *Phys. Rev. Lett.* **99**, 133603 (2007).
- [39] K. B. Davis, M. O. Mewes, M. R. Andrews, N. J. van Druten, D. S. Durfee, D. M. Kurn, and W. Ketterle, *Phys. Rev. Lett.* **75**, 3969 (1995).
- [40] J. Javanainen and S. M. Yoo, *Phys. Rev. Lett.* **76**, 161 (1996).
- [41] M. Naraschewski, H. Wallis, A. Schenzle, J. I. Cirac, and P. Zoller, *Phys. Rev. A* **54**, 2185 (1996).
- [42] M. R. Andrews, C. G. Townsend, H. J. Miesner *et al.*, *Science* **275**, 637 (1997).